Phase sensitivity at the Heisenberg limit in an SU(1,1) interferometer via parity detection

Dong Li,[1,2] Bryan T. Gard,[2] Yang Gao,[3] Chun-Hua Yuan,[1,4,*] Weiping Zhang,[4,5] Hwang Lee,[2,†] and Jonathan P. Dowling[2]

[1]*Quantum Institute for Light and Atoms, Department of Physics, East China Normal University, Shanghai 200062, People's Republic of China*

[2]*Hearne Institute for Theoretical Physics and Department of Physics and Astronomy, Louisiana State University, Baton Rouge, Louisiana 70803, USA*

[3]*Department of Physics, Xinyang Normal University, Xinyang, Henan 464000, People's Republic of China*

[4]*Collaborative Innovation Center of Extreme Optics, Shanxi University, Taiyuan, Shanxi 030006, People's Republic of China*

[5]*Department of Physics and Astronomy, Shanghai Jiao Tong University, Shanghai 200240, People's Republic of China*

We theoretically investigate the phase sensitivity with parity detection on an SU(1,1) interferometer with a coherent state combined with a squeezed vacuum state. This interferometer is formed with two parametric amplifiers for beam splitting and recombination instead of beam splitters. We show that the sensitivity of phase estimation approaches the Heisenberg limit and give the corresponding optimal condition. Moreover, we derive the quantum Cramér-Rao bound of the SU(1,1) interferometer.

I. INTRODUCTION

High-precision metrology has recently been receiving a lot of attention [1–4] due to the benefits to advanced science and technology. One common tool for high-precision measurement is the optical Mach-Zehnder interferometer (MZI), which typically contains two beam splitters (BS). Usually coherent light is split by the first BS, then one beam experiences a phase shift ϕ while the other is retained as a reference, and the two beams combine by a second BS. One can detect the output light to obtain the phase shift information. However the phase sensitivity $\Delta\phi$ is limited by the shot noise limit (SNL), $1/\sqrt{\bar{n}}$ ($\bar{n}$ is the total mean photon number). This limit is due to the classical nature of the coherent state and can be surpassed by using nonclassical states of light, such as squeezed states [5] and NOON states [6,7]. With the help of the nonclassical states, the phase sensitivity can achieve the Heisenberg limit (HL).

Another possibility for beating the SNL is to use an interferometer in which the mixing of the optical beams is done through a nonlinear transformation, such as the SU(1,1) interferometer as shown in Fig. 1. This type of interferometer, first proposed by Yurke *et al.* [8], is described by the group SU(1,1), as opposed to the SU(2) Mach-Zehnder one, where nonlinear transformations are optical parametric amplifiers (OPAs) or four-wave mixers. Yurke *et al.* [8] pointed out that this type of interferometer with vacuum inputs has a phase sensitivity $1/[\bar{n}(\bar{n}+2)]^{1/2}$, where $\bar{n}$ is the total mean photon number inside the interferometer and is equal to $2\sinh^2 g$, with g as the OPA strength. However, $\bar{n}$ is small because the photon number in this scheme is only related to the OPA strength g, which is of order of 3 available currently [9,10]. This phase sensitivity has been also discussed in Refs. [11,12].

Recently, a new theoretical scheme was proposed to inject strong coherent light to "boost" the photon number in an SU(1,1) interferometer with intensity detection by Plick *et al.* [13]. Their scheme circumvents the small-photon-number

problem. Jing *et al.* [14] reported the experimental realization of such an interferometer. In this nonlinear interferometer, the maximum output intensity can be much higher than the input due to the parametric amplification. Marino *et al.* [15] investigated the loss effect on phase sensitivity of the SU(1,1) interferometers with intensity detection. They showed that although propagation losses degrade the phase sensitivity, it is still possible to beat the SNL even with a significant amount of loss. Hudelist *et al.* [10] observed an improvement of 4.1 dB in signal-to-noise ratio compared with an SU(2) interferometer under the same operation conditions. More recently, Li *et al.* [16] showed that an SU(1,1) interferometer with coherent and squeezed input states via homodyne detection can approach the HL.

All of the SU(1,1) interferometer schemes mentioned above involve the all-optical nonlinear process as beam splitter. By contrast, experimental realization of the SU(1,1) all-atomic [17–21] and atom-light hybrid [22] interferometers have been also reported, respectively. Gabbrielli *et al.* [21] presented a nonlinear three-mode SU(1,1) atomic interferometer realized with ultracold atoms. Chen *et al.* [22] reported an SU(1,1) atom-light hybrid interferometer utilizing the interface between the light and collective atomic excitation. Furthermore, the SU(1,1)-type interferometer was also proposed in the circuit quantum electrodynamics system [23], which provides a different method for basic measurement.

Heisenberg-limited sensitivity of phase estimation is one goal of quantum optical metrology. For this purpose, the search for the optimal detection scheme still continues. Here, we consider parity measurement as our detection scheme. Parity detection was first proposed by Bollinger *et al.* [6] in 1996 to study spectroscopy with a maximally entangled state of trapped ions. It was later adopted for an optical interferometer by Gerry [24]. Mathematically, parity detection is described by a simple single-mode operator $\hat{\Pi} = (-1)^{\hat{N}}$, where $\hat{N}$ is the photon-number operator. Hence, parity is simply the evenness or oddness of the photon number in an output mode. In experiments, the parity operator can be implemented by using homodyne techniques [25] for high power, or observing the photon-number distribution with a photon-number resolving detector for small photon numbers.
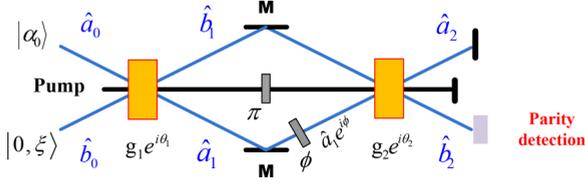
FIG. 1. The schematic diagram of an SU(1,1) interferometer. Two OPAs take the place of two beam splitters in the traditional Mach-Zehnder interferometer. g_1 (g_2) and θ_1 (θ_2) describe the strength and phase shift in the OPA process 1 (2), respectively. a_i and b_i ($i = 0,1,2$) denote two light beams in the different processes. The pump field between the two OPAs has a π phase difference. ϕ: phase shift; M: mirrors.

Here, we still consider input with coherent $|\alpha_0 = |\alpha_0|e^{i\theta_\alpha}\rangle$ (θ_α is the initial phase of input coherent state) and squeezed vacuum light $|0,\xi = re^{i\theta_s}\rangle$ (r and θ_s are parameters) as in the previous work [16] which focuses on homodyne detection on SU(1,1) interferometers. With coherent and squeezed vacuum light as inputs, one can reduce the required intensity of input coherent states and obtain the same interferometric sensitivity, which can eliminate the disadvantages due to using strong coherent states. Furthermore, as shown in Ref. [16], these input states in an SU(1,1) interferometer are shown to approach the HL when the mean photon numbers in the coherent state and squeezed vacuum state are roughly equal under the condition of OPA process with a strength g in the limit of $e^{-g} \to 0$. This optimal condition for SU(1,1) interferometers is similar to the SU(2) case [26]. For an MZI injected by coherent and squeezed vacuum light, the phase sensitivity with parity detection is $1/\sqrt{|\alpha_0|^2 e^{2r} + \sinh^2 r}$. When the coherent input state and squeezed vacuum input state have a roughly equal intensity, the phase sensitivity reaches the HL.

In this paper, we study parity detection on an SU(1,1) interferometer with coherent and squeezed vacuum input states. Compared with homodyne detection and intensity detection, parity detection has a slightly better phase sensitivity. We also compared the phase sensitivity with another quantum limit, the quantum Cramér-Rao bound (QCRB) [1,27], which sets the ultimate limit for a set of probabilities that originated from measurements on a quantum system. The QCRB is asymptotically achieved by the maximum likelihood estimator and gives a detection-independent phase sensitivity $\Delta\phi_{\text{QCRB}}$.

This paper is organized as follows: In Sec. II we first present the propagation of input fields through the SU(1,1) interferometer. Then we discuss the HL in an SU(1,1) interferometer and compare the phase sensitivity with the HL and the QCRB in Sec. III. Last, we conclude with a summary.

II. PARITY DETECTION ON AN SU(1,1) INTERFEROMETER

A. Model

Figure 1 presents the model of an SU(1,1) interferometer in which the OPAs replace the 50:50 beam splitters in a traditional MZI. Here we consider a coherent light mixed with a squeezed vacuum light as input. $\hat{a}(\hat{a}^\dagger)$ and $\hat{b}$ ($\hat{b}^\dagger$) are the annihilation

(creation) operators corresponding to the two modes a and b. After the first OPA, mode b is retained as a reference, while mode a experiences a phase shift ϕ. After the two modes recombine in the second OPA, the outputs of the two modes are dependent on the phase difference ϕ.

Next, we will focus on the evolution of the input state through an SU(1,1) interferometer in phase space. The Wigner function of the input state, a product state $|\alpha_0\rangle \otimes |0,\xi = re^{i\theta_s}\rangle$, with coherent light amplitude $\alpha_0 = |\alpha_0|e^{i\theta_\alpha}$ and squeezed vacuum with parameters r and θ_s, is given by

$$W_{\text{in}}(\alpha_i,\alpha_0;\beta_i,r) = W_{|\alpha_0\rangle}(\alpha_i,\alpha_0)W_{|0,\xi\rangle}(\beta_i,r), \quad (1)$$

where $W_{\text{in}}(\alpha_i,\alpha_0;\beta_i,r)$ plays the role of quasiprobability density for the complex variables α_i and β_i corresponding to the input beams in mode a and b, respectively. The corresponding Wigner functions of a coherent and squeezed vacuum state can be described as [28]

$$W_{|\alpha_0\rangle}(\alpha_i,\alpha_0) = \frac{2}{\pi}e^{-2|\alpha_i-\alpha_0|^2}, \quad (2)$$

$$W_{|0,\xi\rangle}(\beta_i,r) = \frac{2}{\pi}e^{-2|\beta_i|^2\cosh 2r+(\beta_i^2+\beta_i^{*2})\sinh 2r}, \quad (3)$$

where β_i^* is the conjugate of β_i, and θ_s has been set to zero by appropriately fixing the irrelevant absolute phase θ_α.

After propagation through the SU(1,1) interferometer the output Wigner function is written as

$$W_{\text{out}}(\alpha_f,\beta_f) = W_{\text{in}}[\alpha_i(\alpha_f,\beta_f),\beta_i(\alpha_f,\beta_f)], \quad (4)$$

where α_f and β_f are the variables related to the output beams in modes a and b, respectively, and the relation between variables is described by

$$\begin{pmatrix} \alpha_i \\ \beta_i^* \end{pmatrix} = T^{-1}\begin{pmatrix} \alpha_f \\ \beta_f^* \end{pmatrix}, \quad (5)$$

where β_f^* are the conjugate of β_f. Generally, the propagation through the first OPA, phase shift, and second OPA is described by

$$T = T_{\text{OPA2}}T_\phi T_{\text{OPA1}}, \quad (6)$$

where

$$T_{\text{OPA1}} = \begin{pmatrix} u_1 & v_1 \\ v_1^* & u_1 \end{pmatrix}, \quad (7)$$

$$T_\phi = \begin{pmatrix} e^{i\phi} & 0 \\ 0 & 1 \end{pmatrix}, \quad (8)$$

$$T_{\text{OPA2}} = \begin{pmatrix} u_2 & v_2 \\ v_2^* & u_2 \end{pmatrix}. \quad (9)$$

Here $u_j = \cosh g_j$, $v_j = e^{i\theta_j}\sinh g_j$, and v_j^* is a conjugate of v_j, where θ_j and g_j are the phase shift and parametric strength in the OPA process j ($j = 1,2$), respectively (see, for example, Ref. [29]). More specifically, we assume that the first OPA and the second have a π phase difference (particularly $\theta_1 = 0$ and $\theta_2 = \pi$) and the same parametric strength ($g_1 = g_2 = g$). In such a case, the second OPA will undo what the first one does (namely, $\hat{a}_2 = \hat{a}_0$ and $\hat{b}_2 = \hat{b}_0$) when phase shift $\phi = 0$, which we call a balanced situation.

Combined with Eqs. (5)–(9), the input-output relation of variables has the following form:

$$\alpha_i \rightarrow G\alpha_f + R\beta_f^*, \tag{10}$$

$$\beta_i^* \rightarrow -R\alpha_f + H\beta_f^*, \tag{11}$$

where $G = A - iB\cosh(2g), H = A + iB\cosh(2g)$, and $R = -iB\sinh(2g)$ with $A = \cos(\phi/2)e^{-i\phi/2}$ and $B = \sin(\phi/2)e^{-i\phi/2}$. Therefore, the output Wigner function of a nonlinear interferometer is described by

$$W_{\text{out}}(\alpha_f, \beta_f) = \frac{4}{\pi^2} e^{-2|G\alpha_f + R\beta_f^* - \alpha_0|^2} e^{-2|-R\alpha_f + H\beta_f^*|^2 \cosh(2r)}$$
$$\times e^{2\operatorname{Re}[(-R\alpha_f + H\beta_f^*)^2]\sinh(2r)}. \tag{12}$$

B. Phase sensitivity

Parity measurement has been proved to be an efficient method of detection in interferometer for a wide range of input states [30–33]. For many input states, parity does as well, or nearly as well, as state-specific detection schemes [34,35]. Furthermore, as has been reported recently, parity detection with a two-mode, squeezed vacuum interferometer actually reaches below the phase sensitivity of $1/\bar{n}$ scaling, achieving the QCRB [11].

In this paper, we consider parity detection as our measuring method. The parity operator detection on output mode b is $\hat{\Pi}_b \equiv (-1)^{\hat{b}_2^\dagger \hat{b}_2}$. From the Wigner function, the parity signal is given by [36]

$$\langle \hat{\Pi}_b \rangle = \frac{\pi}{2} \int W_{\text{out}}(\alpha_f, 0) d^2\alpha_f. \tag{13}$$

In our case, $\langle \hat{\Pi}_b \rangle$ is a series of rather complex and unilluminating expressions which are shown in Appendix A.

The sensitivity of phase estimation based on the outcome of the parity detection is estimated as

$$\Delta\phi = \frac{\langle \Delta\hat{\Pi}_b \rangle}{\left| \frac{\partial \langle \hat{\Pi}_b \rangle}{\partial \phi} \right|}, \tag{14}$$

which is a ratio of detection noise to the rate at which signal changes as a function of phase, $\langle \Delta\hat{\Pi}_b \rangle \equiv (\langle \hat{\Pi}_b^2 \rangle - \langle \hat{\Pi}_b \rangle^2)^{1/2} = (1 - \langle \hat{\Pi}_b \rangle^2)^{1/2}$.

The phase sensitivity with parity detection for an SU(1,1) interferometer with coherent and squeezed vacuum states is found to be minimal at $\phi = 0$ and is given by

$$\Delta\phi = \frac{1}{\{N_\alpha[\sinh(2r)\cos(2\theta_\alpha) + \cosh(2r)] + N_s + 1\}^{1/2}}$$
$$\times \frac{1}{[N_{\text{OPA}}(N_{\text{OPA}} + 2)]^{1/2}}, \tag{15}$$

where $N_\alpha = |\alpha_0|^2$ is the intensity of input coherent light, $N_s = \sinh^2 r$ is the intensity of the input squeezed vacuum light, and $N_{\text{OPA}} = 2\sinh^2 g$ is the spontaneous photon number emitted from the first OPA, which is related to parametric strength. When $\theta_\alpha = 0$, the optimal phase sensitivity is found

to be

$$\Delta\phi = \frac{1}{[(N_\alpha e^{2r} + N_s + 1)N_{\text{OPA}}(N_{\text{OPA}} + 2)]^{1/2}}, \tag{16}$$

where the factor e^{2r} results from the input squeezed vacuum beam. If vacuum input is injected ($N_s = 0$ and $N_\alpha = 0$), the phase sensitivity with parity detection is reduced to $\Delta\phi_V = 1/\sqrt{N_{\text{OPA}}(N_{\text{OPA}} + 2)}$, which is the same as the result of Yurke's scheme with intensity detection [8].

III. DISCUSSION

A. Heisenberg limit

In this section, we compare the optimal phase sensitivity of parity detection with the HL. According to Ref. [15], the
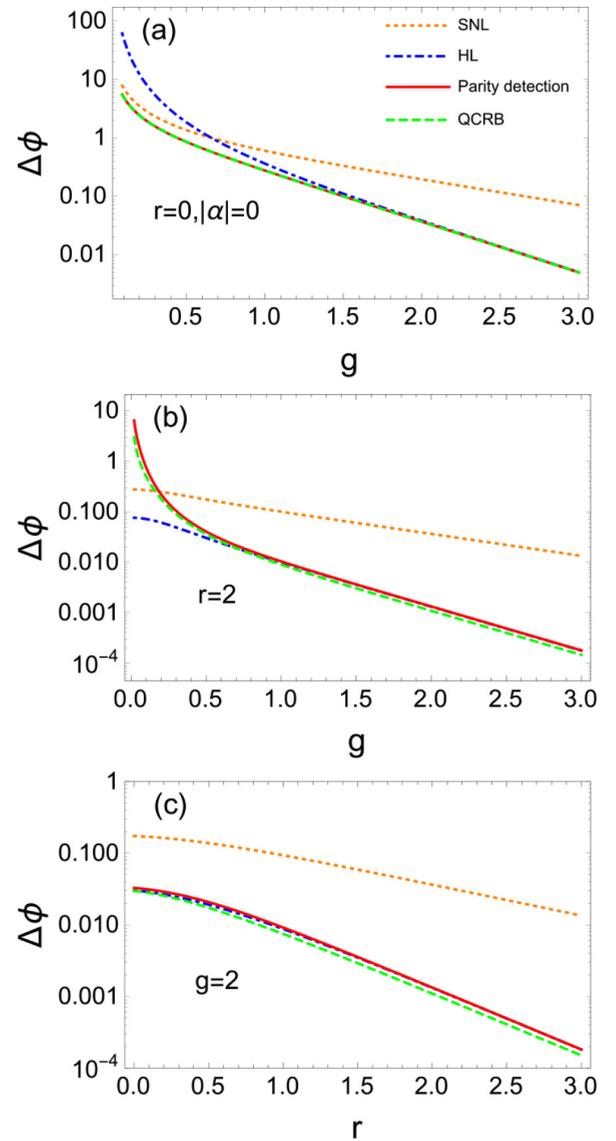

FIG. 2. Sensitivity of phase estimation with parity detection as a function of (a) g with vacuum input $r = 0$ and $|\alpha| = 0$, (b) g with $r = 2$ and $|\alpha_0| = \tanh(2g)e^r/2$, and (c) r with $g = 2$ and $|\alpha_0| = \tanh(2g)e^r/2$. The dotted-orange line is for the SNL, the dash-dotted-blue is for the HL, the dashed-green is for the QCRB, and the solid-red is for the phase sensitivity with parity detection.

corresponding HL is related to the total number of photons $N_{\text{Tot}}(\equiv \langle \hat{a}_1^\dagger \hat{a}_1 + \hat{b}_1^\dagger \hat{b}_1 \rangle)$ inside the SU(1,1) interferometer, not the input photon number as the traditional MZI. This is due to amplification of the phase-sensing photon number by the first OPA. Then the HL is given by

$$\Delta \phi_{\text{HL}} = \frac{1}{N_{\text{Tot}}}, \tag{17}$$

where the subscript HL represents the Heisenberg limit. According to Ref. [16], the total inside photon number is

$$N_{\text{Tot}} = (N_{\text{OPA}} + 1)(N_\alpha + N_s) + N_{\text{OPA}}, \tag{18}$$

where the first term on the right-hand side, $(N_{\text{OPA}} + 1)(N_\alpha + N_s)$, results from the amplification process of the input photon number and the second one is only related to OPA strength g, which corresponds to amplification of the vacuum input state or the so-called spontaneous process. Thus the total inside photon number N_{Tot} corresponds to not only the OPA strength but also input photon number.

When vacuum input is injected, the Heisenberg limit is found to be $\Delta \phi_{\text{HL}} = 1/N_{\text{Tot}} = 1/N_{\text{OPA}}$, while the corresponding phase sensitivity with parity detection is $\Delta \phi_{\text{V}} = 1/\sqrt{N_{\text{OPA}}(N_{\text{OPA}} + 2)}$. Figure 2(a) compares the phase sensitivity $\Delta \phi_{\text{V}}$ with the HL and the SNL, as a function of OPA strength g, under the condition of vacuum input. It reveals that parity detection can achieve the HL. With the increase of g, the phase sensitivity $\Delta \phi$ becomes more and more close to the HL. We notice that the SNL is below the HL when $g \lesssim 0.6$, which is due to the total inside photon number $N_{\text{Tot}} < 1$.

Next, we consider coherent and squeezed vacuum input states. Comparing Eq. (16) with Eq. (17), the necessary optimal condition for approaching HL in the limit of $e^{-r} \to 0$ and $e^{-g} \to 0$ is found to be [37]

$$|\alpha_0| \simeq \frac{\tanh(2g)e^r}{2}. \tag{19}$$

This expression reveals the requirement for the input coherent state $|\alpha_0|$, the input squeezed vacuum state r, and the OPA process g. When $\tanh(2g) \simeq 1$, Eq. (19) is simplified to $N_\alpha \simeq e^{2r}/4 \simeq \sinh^2 r = N_s$. The total photon number of Eq. (18) simplifies to $N_{\text{Tot}} \simeq 2N_{\text{OPA}}N_\alpha$. Then under the condition of $\tanh(2g) \simeq 1$, the phase sensitivity $\Delta \phi$ with parity detection of Eq. (16) always approaches the HL of Eq. (17), which is

given by

$$\Delta \phi \simeq \frac{1}{\sqrt{4N_\alpha^2 N_{\text{OPA}}^2}} \simeq \frac{1}{N_{\text{Tot}}}. \tag{20}$$

Similar to the MZI, it requires the photon numbers in two input ports of the SU(1,1) interferometer to be balanced to approach the HL [38]. We plot the phase sensitivity $\Delta \phi$ as a function of OPA strength g in Fig. 2(b), which presents the comparison between $\Delta \phi$ and $\Delta \phi_{\text{HL}}$. Under the condition $r = 2$ and $|\alpha_0| = \tanh(2g)e^r/2$, the phase sensitivity approaches the HL when $g > 2$ [$\tanh(2g) \simeq 1$]. When $g < 1$, increasing the input squeezed parameter r and increasing the input coherent mean photon number enables the phase sensitivity to beat the SNL, but it does not approach the HL. Figure 2(c) is a plot of the phase sensitivity $\Delta \phi$ as a function of input squeezed parameter r. Given $g = 2$ and $|\alpha_0| = \tanh(2g)e^r/2$, the phase sensitivity is always below the SNL and close to the HL.

B. Quantum Cramér-Rao bound

So far, we have shown that parity detection can approach the phase sensitivity of scaling of $1/N_{\text{Tot}}$ in the SU(1,1) interferometer with coherent and squeezed vacuum input states. In this section we will investigate the QCRB of an SU(1,1) interferometer and compare the optimal phase sensitivity by parity detection with the QCRB, which gives an upper limit to the precision of quantum parameter estimation. We also compare parity detection with homodyne detection and intensity detection.

Recently, Gao *et al.* [39] developed a general formalism for the QCRB of Gaussian states, in which the QCRB can be fully expressed in terms of the mean displacement and covariance matrix of the Gaussian state. Here, we utilize this method to obtain the QCRB of our interferometric scheme. The QCRB for an SU(1,1) interferometer with coherent and squeezed vacuum input is found to be (see Appendix B for details)

$$\Delta \phi_{\text{QCRB}} = (2N_\alpha(N_{\text{OPA}} + 2)\{N_{\text{OPA}}[N_s + \sqrt{N_s(N_s + 1)} + 1]\} + N_{\text{OPA}}[N_{\text{OPA}}(2N_s + 1) + 2](N_s + 1))^{-1/2}, \tag{21}$$

where the term on the right-hand side shows that $\Delta \phi_{\text{QCRB}}$ is related to not only the input coherent intensity and the input squeezed vacuum intensity, but also the optical parametric strength.

TABLE I. The phase sensitivity with various detections and QCRB of an SU(1,1) interferometer with different input states.

Input states	Parity	Homodyne	Intensity	QCRB
$\lvert 0 \rangle \otimes \lvert 0 \rangle$	$1/\mathcal{K}^{1/2}$	Not available [40]	$1/\mathcal{K}^{1/2}$	$1/\mathcal{K}^{1/2}$
$\lvert \alpha_0 \rangle \otimes \lvert 0 \rangle$	$1/[\mathcal{K}(N_\alpha + 1)]^{1/2}$	$1/[\mathcal{K}N_\alpha]^{1/2}$ [16]	$\Delta \phi_{\text{I,coh}}$[a]	$1/[\mathcal{K}(2N_\alpha + 1) + 2N_\alpha(N_{\text{OPA}} + 2)]^{1/2}$
$\left\lvert \frac{i\alpha_0}{\sqrt{2}} \right\rangle \otimes \left\lvert \frac{\alpha_0}{\sqrt{2}} \right\rangle$	$\Delta \phi_{\text{coh}}$[b]	$\approx 1/[2\mathcal{K}N_\alpha]^{1/2}$ [16]	$1/[\mathcal{K}N_\alpha]^{1/2}$ [13]	$1/\{2N_\alpha[(N_{\text{OPA}} + 1)\sqrt{\mathcal{K}} + \mathcal{K} + 1] + \mathcal{K}\}^{1/2}$
$\lvert \alpha_0 \rangle \otimes \lvert 0, \xi \rangle$	$1/[\mathcal{K}(N_\alpha e^{2r} + \cosh^2 r)]^{1/2}$	$1/[\mathcal{K}N_\alpha e^{2r}]^{1/2}$ [16]	$\Delta \phi_{\text{I,coh\&sqz}}$[c]	$1/[2N_\alpha(N_{\text{OPA}} + 2) + N_{\text{OPA}}^2 \sinh^2(2r)/2 + \mathcal{K}(2N_\alpha \cosh r e^r + \cosh^2 r)]^{1/2}$

$\mathcal{K} = N_{\text{OPA}}(N_{\text{OPA}} + 2)$. Row 1: vacuum input state; row 2: one coherent input state; row 3: two coherent input states; row 4: coherent mixed with squeezed vacuum input state.

[a]See Appendix C.
[b]See Appendix D.
[c]See Appendix C.

TABLE II. The QCRB of an MZI with different input states.

Input states	Parity	QCRB
$\lvert \alpha_0 \rangle \otimes \lvert 0 \rangle$	$1/\sqrt{N_\alpha}$	$1/\sqrt{N_\alpha}$
$\lvert i\frac{\alpha_0}{\sqrt{2}} \rangle \otimes \lvert \frac{\alpha_0}{\sqrt{2}} \rangle$	Not available [41]	$1/\sqrt{N_\alpha}$
$\lvert \alpha_0 \rangle \otimes \lvert 0, \xi = re^{i\theta_s} \rangle$	$1/\sqrt{N_\alpha e^{2r} + \sinh^2 r}$ [26]	$1/\sqrt{N_\alpha e^{2r} + \sinh^2 r}$ [38]

$N_\alpha = |\alpha_0|^2$ is the mean photon number. Row 1: one coherent input state; row 2: two equal coherent input states; row 3: coherent mixed with squeezed vacuum input state.

Table I shows the QCRB with four different Gaussian input states. For vacuum input ($r = 0$, $N_\alpha = 0$), the QCRB is reduced to $\Delta\phi_{QCRB} = 1/\sqrt{N_{OPA}(N_{OPA} + 2)}$, and it can be saturated by parity detection and intensity detection. However, in this case the phase sensitivity of homodyne detection with vacuum input is not available due to its measurement signal being a constant 0 independent of phase shift ϕ [40]. With the other three nonvacuum input states, the QCRB can be approached but not be reached with these three detection methods, as shown in Table I.

Table II presents the comparison between phase sensitivity with parity detection and the QCRB in an SU(2) interferometer with various inputs. For two equal coherent input states, parity detection has poor statistics [41]. However parity detection achieves the QCRB with only one coherent state input or coherent mixed with squeezed vacuum state input. However, we notice that parity detection on an SU(1,1) interferometer does not reach the QCRB with the same inputs. According to Tables I and II, the SU(1,1) interferometer has a better phase sensitivity than the MZI by roughly a factor of $\sqrt{N_{OPA}(N_{OPA} + 2)}$ with one coherent input $\lvert \alpha_0 \rangle \otimes \lvert 0 \rangle$ and coherent mixed with squeezed vacuum input $\lvert \alpha_0 \rangle \otimes \lvert 0, \xi \rangle$ due to the amplification process.

Next, we compare the optimal phase sensitivities among the parity detection, homodyne detection, and intensity detection in the SU(1,1) interferometer. For the coherent $\otimes$ squeezed vacuum state input or only one coherent state input, the phase sensitivities of these three methods have similar results because the phase sensitivity of the coherent $\otimes$ squeezed vacuum state input can reduce to only one coherent state input when $r = 0$. The expressions of phase sensitivity with intensity detection are complex, as shown in Appendix C. Figures 3(a) and 3(b) show the phase sensitivities with intensity detection as a function of ϕ with coherent and squeezed vacuum state input and only one coherent state input, respectively. For these two cases, the optimal phase points are both very close to zero. Figures 3(d) and 3(e) plot the corresponding optimal phase sensitivities as a function of g, in which the optimal phase sensitivities become better with the increase of g. The optimal phase sensitivity by parity detection is slightly better than that of homodyne detection, and the phase sensitivity by intensity detection is the worst among them.

For two-equal coherent input states $\lvert i\alpha_0/\sqrt{2} \rangle \otimes \lvert \alpha_0/\sqrt{2} \rangle$, the expression of the phase sensitivity with parity detection is very complex, as shown in Appendix D. Figure 3(c) presents the phase sensitivity with parity detection as a function of ϕ. It shows that the optimal phase point is also close to zero. Figure 3(f) plots the optimal phase sensitivity verse g. In such a situation, the phase sensitivities by homodyne detection and by parity detection are the best and the worst, respectively.
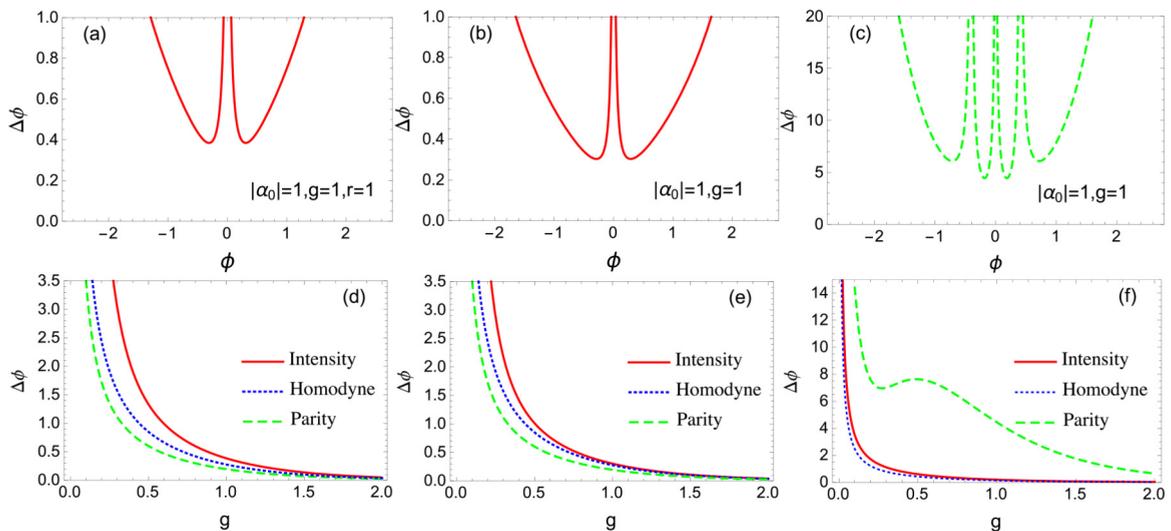

FIG. 3. The sensitivity of phase estimation of an SU(1,1) interferometer as a function of (a) ϕ with intensity detection with coherent and squeezed vacuum input state with $r = 1$; (b) ϕ with intensity detection with only one coherent input state; and (c) ϕ with parity detection with two equal coherent input state. The optimal phase sensitivity of an SU(1,1) interferometer versus (d) g with coherent and squeezed vacuum input state with $r = 1$; (e) g with only one coherent input state; and (f) g with two equal coherent input states (the blue line is for optimal phase sensitivity and the dashed-red line is for phase sensitivity at $\phi = \phi_{opt}$). Parameter: $|\alpha_0| = 1$.

IV. CONCLUSION

In summary, we have investigated the parity detection on an SU(1,1) interferometer with pure Gaussian states as inputs. We have presented that parity detection approaches the phase sensitivity of $1/N_{\text{Tot}}$ scaling when the coherent beam and squeezed vacuum beam have a roughly equal intensity with a parametric strength in the limit of $e^{-g} \to 0$. Compared with homodyne detection and intensity detection, parity detection has a slightly better optimal phase sensitivity with only one coherent state input or coherent and squeezed vacuum input states. However, with two equal coherent state inputs, parity detection cannot give better results than homodyne detection and intensity detection. We have also shown a brief study of the QCRB of an SU(1,1) interferometer. With vacuum input, the QCRB is saturated by parity detection. However, parity detection does not saturate the QCRB as well as homodyne detection and intensity detection with the three nonvacuum inputs in Table I. This motivates us to look for new optimal detection schemes to approach the QCRB in future work.

APPENDIX A: PARITY DETECTION SIGNAL

From Eqs. (12) and (13), the measurement signal $\langle \hat{\Pi}_b \rangle$ is found to be

$$\langle \hat{\Pi}_b \rangle = \frac{1}{\sqrt{T_1}} e^{-T_2/T_3}, \tag{A1}$$

where

$$\begin{aligned} T_1 &= e^{-2r}(e^{2r}+1)^2 \{8\sinh^4(2g)[\cos(2\phi)-\cos\phi] \\ &\quad + 4\cosh(4g) + 3\cosh(8g) - 7\} + 64, \\ T_2 &= 4|\alpha_0|^2 \sinh^2(2g)\{8\cosh(4g)\cos(2\theta_\alpha)\sin^4(\phi/2) \\ &\quad - 8\cosh(2g)\sin(2\theta_\alpha)\sin\phi(\cos\phi-1) \\ &\quad + 8e^{4r}[\cos\theta_\alpha\sin\phi - 2\cosh(2g)\sin\theta_\alpha\sin^2(\phi/2)]^2 \\ &\quad + 32e^{2r}\sinh^2(2g)\sin^4(\phi/2) \\ &\quad + 8\cosh(4g)\sin^4(\phi/2) - 8\cos^2\theta_\alpha\cos\phi \\ &\quad + [3\cos(2\theta_\alpha) - 1]\cos(2\phi) + \cos(2\theta_\alpha) + 5\}, \\ T_3 &= (e^{2r}+1)^2[8\cosh(8g)\sin^4(\phi/2) + 8\cosh(4g)\sin^2\phi \\ &\quad + 4\cos\phi + 3\cos(2\phi) - 7] + 64e^{2r}. \end{aligned}$$

Letting $\phi = 0$, we find that signal is reduced to

$$\langle \hat{\Pi}_b \rangle|_{\phi=0} = 1, \tag{A2}$$

which matches our prediction. When $\phi = 0$, the second OPA would undo what the first one does, causing the output fields to be the same as the inputs. Thus the output in mode b is the one-mode squeezed vacuum. For the one-mode squeezed vacuum, parity signal is 1 due to only even number distribution in the Fock basis with $|0,\xi = re^{i\theta_s}\rangle = \sqrt{1/\cosh r} \sum_{n=0}^{\infty} [\sqrt{(2n)!}/n](1/2)^n [\exp(i\theta_s) \tanh r]^n |2n\rangle$ [42].

APPENDIX B: QUANTUM CRAMÉR-RAO BOUND

First we will focus on evolution of mean values and the covariance matrix of quadrature operators in an SU(1,1) interferometer. Second we will transform from the quadrature operator basis to the annihilation (creation) operator basis. Then according to Ref. [39], the QCRB will be obtained by mean values and a covariance matrix of annihilation (creation) operators.

$\hat{a}_i$ ($\hat{a}_i^\dagger$) and $\hat{b}_i$ ($\hat{b}_i^\dagger$) ($i = 0,1,2$) are the annihilation (creation) operators as shown in Fig. 1. We introduce the quadrature operators

$$\begin{aligned} \hat{x}_{a_i} &= \hat{a}_i + \hat{a}_i^\dagger, \quad \hat{p}_{a_i} = -i(\hat{a}_i - \hat{a}_i^\dagger), \\ \hat{x}_{b_i} &= \hat{b}_i + \hat{b}_i^\dagger, \quad \text{and} \quad \hat{p}_{b_i} = -i(\hat{b}_i - \hat{b}_i^\dagger). \tag{B1} \end{aligned}$$

We also define quadrature column vector

$$\mathbf{X}_i = (\hat{X}_{i,1}, \hat{X}_{i,2}, \hat{X}_{i,3}, \hat{X}_{i,4})^\mathsf{T} \equiv (\hat{x}_{a_i}, \hat{p}_{a_i}, \hat{x}_{b_i}, \hat{p}_{b_i})^\mathsf{T}. \tag{B2}$$

Next, we focus on the column vector of expectation values of the quadratures $\bar{\mathbf{X}}_i$ and the symmetrized covariance matrix Γ_i [39,43–45], where

$$\bar{\mathbf{X}}_i = (\langle \hat{X}_{i,1} \rangle, \langle \hat{X}_{i,2} \rangle, \langle \hat{X}_{i,3} \rangle, \langle \hat{X}_{i,4} \rangle)^\mathsf{T}, \tag{B3}$$

$$\Gamma_i^{kl} = \tfrac{1}{2}\text{Tr}[(\tilde{X}_{i,k}\tilde{X}_{i,l} + \tilde{X}_{i,l}\tilde{X}_{i,k})\rho], \tag{B4}$$

with $\tilde{X}_{i,k} = \hat{X}_{i,k} - \langle \hat{X}_{i,k} \rangle, \tilde{X}_{i,l} = \hat{X}_{i,l} - \langle \hat{X}_{i,l} \rangle$ and ρ the density matrix.

The input-output relation of $\bar{\mathbf{X}}_i$ and Γ_i can be described as [46]

$$\bar{\mathbf{X}}_2 = S\bar{\mathbf{X}}_0, \tag{B5}$$

$$\Gamma_2 = S\Gamma_0 S^\mathsf{T}, \tag{B6}$$

where $\bar{\mathbf{X}}_2$ ($\bar{\mathbf{X}}_0$) and $\Gamma_2(\Gamma_0)$ are column vector of expectation values of the quadratures and symmetrized covariance matrix for the output (input) states, respectively, and S is the transformation matrix. In general, transformation through the first OPA, phase shift, and the second OPA could be given by

$$S_{\text{OPA1}} = \begin{pmatrix} \cosh g & 0 & \sinh g & 0 \\ 0 & \cosh g & 0 & -\sinh g \\ \sinh g & 0 & \cosh g & 0 \\ 0 & -\sinh g & 0 & \cosh g \end{pmatrix}, \tag{B7}$$

$$S_\phi = \begin{pmatrix} \cos\phi & -\sin\phi & 0 & 0 \\ \sin\phi & \cos\phi & 0 & 0 \\ 0 & 0 & 1 & 0 \\ 0 & 0 & 0 & 1 \end{pmatrix}, \quad \text{(B8)}$$

$$S_{\text{OPA2}} = \begin{pmatrix} \cosh g & 0 & -\sinh g & 0 \\ 0 & \cosh g & 0 & \sinh g \\ -\sinh g & 0 & \cosh g & 0 \\ 0 & \sinh g & 0 & \cosh g \end{pmatrix}, \quad \text{(B9)}$$

where we have considered the balanced situation that $\theta_1 = 0$, $\theta_2 = \pi$ and $g_1 = g_2 = g$. Therefore, the matrix can be obtained as $S = S_{\text{OPA2}} S_\phi S_{\text{OPA1}}$.

In our case of a coherent and squeezed vacuum input state $(|\alpha_0\rangle \otimes |0, \xi = re^{i\theta_s}\rangle)$, the initial mean value of quadrature vector $\bar{\mathbf{X}}_0$ and covariance matrix Γ_0 are

$$\bar{\mathbf{X}}_0 = (2|\alpha_0|\,0\,0\,0)^\mathsf{T}, \quad \text{(B10)}$$

$$\Gamma_0 = \begin{pmatrix} 1 & 0 & 0 & 0 \\ 0 & 1 & 0 & 0 \\ 0 & 0 & e^{2r} & 0 \\ 0 & 0 & 0 & e^{-2r} \end{pmatrix}, \quad \text{(B11)}$$

respectively, where we have let $\theta_\alpha = 0$ and $\theta_s = 0$. According to Eqs. (B5) and (B6), the final states can be found to be

$$\bar{\mathbf{X}}_2 = 2|\alpha_0| \begin{pmatrix} \cosh^2 g \cos\phi - \sinh^2 g \\ \cosh^2 g \sin\phi \\ \sinh g \cosh g(1 - \cos\phi) \\ \sinh g \cosh g \sin\phi \end{pmatrix}, \quad \text{(B12)}$$

$$\Gamma_2 = \begin{pmatrix} \gamma_{11} & \gamma_{12} & \gamma_{13} & \gamma_{14} \\ \gamma_{21} & \gamma_{22} & \gamma_{23} & \gamma_{24} \\ \gamma_{31} & \gamma_{32} & \gamma_{33} & \gamma_{34} \\ \gamma_{41} & \gamma_{42} & \gamma_{43} & \gamma_{44} \end{pmatrix}, \quad \text{(B13)}$$

where

$$\gamma_{11} = e^{-2r}(e^{2r}\cos^2\phi \cosh^4 g + \{e^{2r}\cosh^2 r \sin^2\phi + [e^{4r}\cos^2\phi - 2e^{2r}(1 + e^{2r})\cos\phi$$
$$+ e^{4r} + \sin^2\phi]\sinh^2 g\}\cosh^2 g + e^{2r}\sinh^4 g), \quad \text{(B14)}$$

$$\gamma_{12} = e^{-2r}\cosh g \cosh r \sin\phi[e^{2r}\cos\phi \cosh^2 g - e^{2r}\cos\phi \cosh^2 r + (-1 + e^{4r})(\cos\phi - 1)\sinh^2 g]$$
$$= \gamma_{21}, \quad \text{(B15)}$$

$$\gamma_{13} = e^{-2r}\cosh g \sinh g \left\{ e^{2r}(e^{2r} - \cos\phi)(\cos\phi - 1)\cosh^2 g - e^{2r}\cosh^2 r \sin^2\phi \right.$$
$$\left. + 2(1 + e^{2r})[(-1 + e^{2r})\cos\phi - 1]\sin^2\frac{\phi}{2}\sinh^2 g \right\}$$
$$= \gamma_{31}, \quad \text{(B16)}$$

$$\gamma_{14} = e^{-2r}\cosh g \sin\phi \sinh g\{e^{2r}\cos\phi \cosh^2 g + (1 - e^{2r}\cos\phi + e^{2r})\cosh^2 r + (1 + e^{2r})[(-1 + e^{2r})\cos\phi - e^{2r}]\sinh^2 g\}$$
$$= \gamma_{41}, \quad \text{(B17)}$$

$$\gamma_{22} = e^{-2r}(e^{2r}\cos^2\phi \cosh^4 r + \{e^{2r}\cosh^2 g \sin^2\phi + [\cos^2\phi - 2(1 + e^{2r})\cos\phi + e^{4r}\sin^2\phi + 1]\sinh^2 g\}\cosh^2 r + e^{2r}\sinh^4 g),$$
$$\quad \text{(B18)}$$

$$\gamma_{23} = e^{-2r}\cosh r \sin\phi \sinh g\{e^{2r}(-\cos\phi + e^{2r} + 1)\cosh^2 g + e^{2r}\cos\phi \cosh^2 r - (1 + e^{2r})[(-1 + e^{2r})\cos\phi + 1]\sinh^2 g\}$$
$$= \gamma_{32}, \quad \text{(B19)}$$

$$\gamma_{24} = e^{-2r}\cosh r \sinh g \left\{ (\cos\phi - 1)(e^{2r}\cos\phi - 1)\cosh^2 r + e^{2r}\cosh^2 g \sin^2\phi \right.$$
$$\left. + 2(1 + e^{2r})[(-1 + e^{2r})\cos\phi + e^{2r}]\sin^2\frac{\phi}{2}\sinh^2 g \right\}$$
$$= \gamma_{42}, \quad \text{(B20)}$$

$$\gamma_{33} = e^{-2r}\{e^{4r}\cosh^4 g - e^{2r}[-\cos^2\phi + 2(1 + e^{2r})\cos\phi - 1]\sinh^2 g \cosh^2 g + (e^{4r}\cos^2\phi + \sin^2\phi)\sinh^4 g$$
$$+ e^{2r}\cosh^2 r \sin^2\phi \sinh^2 g\}, \quad \text{(B21)}$$

$$\gamma_{34} = -e^{-2r}\sin\phi \sinh^2 g[-e^{2r}(-\cos\phi + e^{2r} + 1)\cosh^2 g + (-e^{2r}\cos\phi + e^{2r} + 1)\cosh^2 r + (-1 + e^{4r})\cos\phi \sinh^2 g]$$
$$= \gamma_{43}, \quad \text{(B22)}$$

and

$$\gamma_{44} = e^{-2r}\{\cosh^4 r + [e^{2r}\cos^2\phi - 2(1 + e^{2r})\cos\phi + e^{2r}]\sinh^2 g \cosh^2 r + (\cos^2\phi + e^{4r}\sin^2\phi)\sinh^4 g$$
$$+ e^{2r}\cosh^2 g \sin^2\phi \sinh^2 g\}. \quad \text{(B23)}$$

So far, we have obtained the output quadrature vector and its covariance matrix. Next, we will calculate the corresponding creation and annihilation operator vector which is defined as

$$\mathbf{d} = (d_1, d_2, d_3, d_4)^{\mathsf{T}} \equiv (\hat{a}_2, \hat{a}_2^{\dagger}, \hat{b}_2, \hat{b}_2^{\dagger})^{\mathsf{T}}, \qquad (B24)$$

and its covariance matrix Σ where each matrix element is defined as

$$\Sigma^{u,v} = (1/2)\text{Tr}[\rho(\tilde{d}_u \tilde{d}_v + \tilde{d}_v \tilde{d}_u)], \qquad (B25)$$

with $\tilde{d}_u = d_u - \bar{d}_u$ in terms of $\bar{d}_u = \text{Tr}[\rho d_u]$ where ρ is the density matrix. The corresponding commutation relation is described as $[d_u, d_v] = \Omega^{u,v}$, where

$$\Omega = \begin{pmatrix} 0 & 1 & 0 & 0 \\ -1 & 0 & 0 & 0 \\ 0 & 0 & 0 & 1 \\ 0 & 0 & -1 & 0 \end{pmatrix}. \qquad (B26)$$

Here we define the expectation value of $\mathbf{d}$ as

$$\bar{\mathbf{d}} \equiv (\bar{d}_1, \bar{d}_2, \bar{d}_3, \bar{d}_4)^{\mathsf{T}} = (\langle\hat{a}_2\rangle, \langle\hat{a}_2^{\dagger}\rangle, \langle\hat{b}_2\rangle, \langle\hat{b}_2^{\dagger}\rangle)^{\mathsf{T}}. \qquad (B27)$$

According to Eqs. (B1)–(B3), $\bar{\mathbf{X}}_2$ is found to be

$$\bar{\mathbf{X}}_2 = (\langle\hat{a}_2 + \hat{a}_2^{\dagger}\rangle, \langle-i(\hat{a}_2 - \hat{a}_2^{\dagger})\rangle, \langle\hat{b}_2 + \hat{b}_2^{\dagger}\rangle, \langle-i(\hat{b}_2 - \hat{b}_2^{\dagger})\rangle)^{\mathsf{T}}. \qquad (B28)$$

Combined with Eqs. (B27) and (B28) the relation between $\bar{\mathbf{d}}$ and $\bar{\mathbf{X}}_2$ is expressed as

$$\bar{\mathbf{d}} = H\bar{\mathbf{X}}_2, \qquad (B29)$$

where

$$H = \frac{1}{2}\begin{pmatrix} 1 & i & 0 & 0 \\ 1 & -i & 0 & 0 \\ 0 & 0 & 1 & i \\ 0 & 0 & 1 & -i \end{pmatrix}. \qquad (B30)$$

Similarly, one can obtain the relation between Σ and Γ_2 as follows:

$$\Sigma = H\Gamma_2 H^{\mathsf{T}}. \qquad (B31)$$

According to Ref. [39], the quantum Fisher information is given by

$$F = \frac{1}{2}\text{Tr}\left\{\partial_{\phi}\Sigma\left[\Sigma(\partial_{\phi}\Sigma)^{-1}\Sigma^{\mathsf{T}} + \frac{1}{4}\Omega(\partial_{\phi}\Sigma)^{-1}\Omega^{\mathsf{T}}\right]^{-1}\right\} + (\partial_{\phi}\bar{\mathbf{d}})^{\mathsf{T}}(\Sigma)^{-1}(\partial_{\phi}\bar{\mathbf{d}}), \qquad (B32)$$

where $\partial_{\phi}\Sigma = \partial\Sigma/\partial\phi$ and $\partial_{\phi}\bar{\mathbf{d}} = \partial\bar{\mathbf{d}}/\partial\phi$. Then the corresponding quantum Cramér-Rao bound [1,27] is given by

$$\Delta\phi_{\text{QCRB}} = \frac{1}{\sqrt{F}}. \qquad (B33)$$

Combined with Eqs. (B12), (B13), (B29), (B31), (B32), and (B33), the QCRB is found to be

$$\Delta\phi_{\text{QCRB}} = (2N_{\alpha}(N_{\text{OPA}} + 2)\{N_{\text{OPA}}[N_s + \sqrt{N_s(N_s + 1)} + 1]\} + N_{\text{OPA}}[N_{\text{OPA}}(2N_s + 1) + 2](N_s + 1))^{-1/2}. \qquad (B34)$$

APPENDIX C: COHERENT STATE AND SQUEEZED VACUUM STATE INPUT WITH INTENSITY DETECTION

The phase sensitivity with intensity detection with coherent and squeezed vacuum input state in an SU(1,1) interferometer is given by

$$\Delta\phi_{\text{I,coh\&sqz}} = \left(\frac{Q_1}{Q_2}\right)^{1/2}, \qquad (C1)$$

where

$$\begin{aligned}Q_1 = &\frac{1}{64}|\alpha_0|^2\{32\sinh^2(2g)\cosh^2(2g)\cosh(2r)\cos(\phi) - 128\sinh^2(2g)\cosh^2(2g)\sinh(2r)\cos(\phi) \\ &- 8\sinh^4(2g)\cosh(2r)\cos(2\phi) + 16\sinh^2(2g)[\cosh(4g) + 3]\sinh(2r)\cos(2\phi) \\ &- 4\cosh(4g)\cosh(2r) - 3\cosh(8g)\cosh(2r) - 16\cosh(4g)\sinh(2r) + 12\cosh(8g)\sinh(2r) \\ &+ 8\sinh^4(2g)\cos(2\phi) - 208\sinh^2(2g)\cos(\phi) - 16\sinh^2(2g)\cosh(4g)\cos(\phi) + 100\cosh(4g) \\ &+ 3\cosh(8g) + 4\sinh(2r) - 57\cosh(2r) + 25\} + \frac{1}{64}\{-64\sinh^2(2g)\cosh^2(2g)\cosh(2r)\cos(\phi) \\ &- 32\sinh^2(2g)\cosh^2(2g)\cosh(4r)\cos(\phi) + 16\sinh^4(2g)\cosh(2r)\cos(2\phi) + 8\sinh^4(2g)\cosh(4r)\cos(2\phi) \\ &+ 8\cosh(4g)\cosh(2r) + 6\cosh(8g)\cosh(2r) + 4\cosh(4g)\cosh(4r) + 3\cosh(8g)\cosh(4r) \\ &- 8\sinh^4(2g)\cos(2\phi) - 48\sinh^2(2g)\cos(\phi) + 16\sinh^2(2g)\cosh(4g)\cos(\phi) + 28\cosh(4g) - 3\cosh(8g) \\ &- 14\cosh(2r) + 9\cosh(4r) - 41\}, \\ Q_2 = &4\sinh^4(g)\cosh^4(g)\sin^2(\phi)[2|\alpha_0|^2 + \cosh(2r) + 1]^2. \qquad (C2)\end{aligned}$$

Figure 3(a) plots the behavior of $\Delta\phi_{\text{I,coh\&sqz}}$ as a function of ϕ with $|\alpha_0| = 1$, $g = 1$, and $r = 1$. It shows that the optimal phase point is close to zero. According to Eq. (C1), the corresponding optimal phase point is found to be

$$\phi_{\text{I,sqz,opt}} = \text{arccot}\left(\sqrt{2^{1/2}V_1 V_2^{-1/2}/8 - 1/2}\right), \qquad (C3)$$

where

$$
\begin{aligned}
V_1 = {} & |-2\cosh(8g)\cosh(2r)|\alpha_0|^2 - 30\cosh(2r)|\alpha_0|^2 + 8\cosh(8g)\sinh(2r)|\alpha_0|^2 - 8\sinh(2r)|\alpha_0|^2 \\
& + 14|\alpha_0|^2 + 16(3|\alpha_0|^2 + 1)\cosh(4g) + 2(|\alpha_0|^2 - 1)\cosh(8g) + 4\cosh(8g)\cosh(2r) \\
& - 4\cosh(2r) + 2\cosh(8g)\cosh(4r) + 6\cosh(4r) - 22|,
\end{aligned}
$$

$$
\begin{aligned}
V_2 = {} & -384|\alpha_0|^4\cosh(4g)\cosh(2r) - 48|\alpha_0|^4\cosh(8g)\cosh(2r) + 8|\alpha_0|^4\cosh(8g)\cosh(4r) \\
& + 128|\alpha_0|^4\cosh(8g)\sinh(2r) - 32|\alpha_0|^4\cosh(8g)\sinh(4r) - 128|\alpha_0|^4\sinh(2r) \\
& + 32|\alpha_0|^4\sinh(4r) - 80|\alpha_0|^4\cosh(2r) + 56|\alpha_0|^4\cosh(4r) - 232|\alpha_0|^4 - 24|\alpha_0|^2\sinh(8g)\sinh(2r) \\
& - 128|\alpha_0|^2\cosh(4g)\cosh(2r) + 74|\alpha_0|^2\cosh(8g)\cosh(2r) + 96|\alpha_0|^2\cosh(4g)\cosh(4r) \\
& + 20|\alpha_0|^2\cosh(8g)\cosh(4r) - 10|\alpha_0|^2\cosh(8g)\cosh(6r) + 8|\alpha_0|^2\cosh(8g)\sinh(6r) \\
& + 24|\alpha_0|^2\sinh(2r) - 8|\alpha_0|^2\sinh(6r) + 86|\alpha_0|^2\cosh(2r) + 12|\alpha_0|^2\cosh(4r) - 22|\alpha_0|^2\cosh(6r) \\
& - 236|\alpha_0|^2 + 32(24|\alpha_0|^4 + 5|\alpha_0|^2 - 1)\cosh(4g) + (40|\alpha_0|^4 - 52|\alpha_0|^2 + 6)\cosh(8g) \\
& - 4\cosh(8g)\cosh(2r) - 8\cosh(8g)\cosh(4r) + 4\cosh(8g)\cosh(6r) + 2\cosh(8g)\cosh(8r) \\
& + 32\cosh(4g)\sinh(4r) + 4\cosh(2r) - 40\cosh(4r) - 4\cosh(6r) + 2\cosh(8r) + 38.
\end{aligned}
\tag{C4}
$$

Inserting $r = 0$ into Eqs. (C1) and (C3), then one obtain the phase sensitivity with only one coherent input state $\Delta\phi_{\mathrm{I,coh}}$ and the corresponding optimal phase point, respectively:

$$
\begin{aligned}
\Delta\phi_{\mathrm{I,coh}} = {} & \{-16\sinh^2(2g)\cos(\phi)[6|\alpha_0|^2 + \cosh(4g) + 3] + 48|\alpha_0|^2\cosh(4g) - 16|\alpha_0|^2 + 8\sinh^4(2g)\cos(2\phi) \\
& + 20\cosh(4g) + 3\cosh(8g) - 23\}|4\sqrt{2}(|\alpha_0|^2 + 1)\sinh^2 2g\sin(\phi)|^{-1},
\end{aligned}
$$

$$
\phi_{\mathrm{I,coh,opt}} = \operatorname{arccot}\left[\sqrt{\frac{4(3|\alpha_0|^2 + 1)\cosh(4g) - 4|\alpha_0|^2 + \cosh(8g) - 5}{8|\alpha_0|\sqrt{4(3|\alpha_0|^2 + 1)\cosh(4g) - 8|\alpha_0|^2 + \cosh(8g) - 5}}} - \frac{1}{2}\right].
\tag{C5}
$$

Figure 3(b) plots the behavior of $\Delta\phi_{\mathrm{I,coh}}$ as a function of ϕ with $|\alpha_0| = 1$ and $g = 1$. It shows that the optimal phase point is also close to zero. And Fig. 3(e) shows the corresponding optimal phase as a function of g with $|\alpha_0| = 1$.

APPENDIX D: TWO EQUAL COHERENT STATE INPUT WITH PARITY DETECTION

The phase sensitivity with two equal coherent state input with parity detection on an SU(1,1) interferometer is given by

$$
\Delta\phi_{\mathrm{coh}} = \frac{4[\cosh^2(2g) - \sinh^2(2g)\cos(\phi)]^2\left\{[\cosh^2(2g) - \sinh^2(2g)\cos(\phi)]^2\exp\left[\frac{4|\alpha_0|^2 e^{-2g}(\sinh(2g)\cos(\phi) + \cosh(2g))}{\cosh^2(2g) - \sinh^2(2g)\cos(\phi)}\right] - 1\right\}^{1/2}}{|\sinh(4g)\sin(\phi)[\sinh(4g) - 4|\alpha_0|^2] - 2\sinh^4(2g)\sin(2\phi)|}.
\tag{D1}
$$

Figure 3(c) plots the behavior of $\Delta\phi_{\mathrm{coh}}$ as a function of ϕ with $|\alpha_0| = 1$ and $g = 1$. It shows that the optimal phase point is close to zero. Figure 3(f) compares the optimal phase sensitivity among parity detection, homodyne detection, and intensity detection with two equal coherent state input.

[1] C. W. Helstrom, *Quantum Detection and Estimation Theory* (Academic Press, New York, 1976).

[2] S. L. Braunstein and C. M. Caves, Phys. Rev. Lett. **72**, 3439 (1994).

[3] H. Lee, P. Kok, and J. P. Dowling, J. Mod. Opt. **49**, 2325 (2002).

[4] V. Giovannetti, S. Lloyd, and L. Maccone, Science **306**, 1330 (2004); Nature Photon. **5**, 222 (2011).

[5] C. M. Caves, Phys. Rev. D **23**, 1693 (1981).

[6] J. J. Bollinger, W. M. Itano, D. J. Wineland, and D. J. Heinzen, Phys. Rev. A **54**, R4649 (1996).

[7] J. P. Dowling, Contemp. Phys. **49**, 125 (2008).

[8] B. Yurke, S. L. McCall, and J. R. Klauder, Phys. Rev. A **33**, 4033 (1986).

[9] I. N. Agafonov, M. V. Chekhova, and G. Leuchs, Phys. Rev. A **82**, 011801 (2010).

[10] F. Hudelist, J. Kong, C. Liu, J. Jing, Z. Y. Ou, and W. Zhang, Nat. Commun. **5**, 3049 (2014).

[11] P. M. Anisimov, G. M. Raterman, A. Chiruvelli, W. N. Plick, S. D. Huver, H. Lee, and J. P. Dowling, Phys. Rev. Lett. **104**, 103602 (2010).

[12] The MZI with two-mode squeezed-vacuum state input has a similar phase sensitivity with the SU(1,1) interferometer with vacuum state input.

[13] W. N. Plick, J. P. Dowling, and G. S. Agarwal, New J. Phys. **12**, 083014 (2010).

[14] J. Jing, C. Liu, Z. Zhou, Z. Y. Ou, and W. Zhang, Appl. Phys. Lett. **99**, 011110 (2011).

[15] A. M. Marino, N. V. Corzo Trejo, and P. D. Lett, Phys. Rev. A **86**, 023844 (2012).

[16] D. Li, C. H. Yuan, Z. Y. Ou, and W. Zhang, New J. Phys. **16**, 073020 (2014).

[17] D. Linnemann, Master's thesis, University of Heidelberg, 2013.

[18] D. Linnemann, H. Strobel, W. Muessel, J. Schulz, R. J. Lewis-Swan, K. V. Kheruntsyan, and M. K. Oberthaler, Phys. Rev. Lett. **117**, 013001 (2016).

[19] C. Gross, T. Zibold, E. Nicklas, J. Estève, and M. K. Oberthaler, Nature (London) **464**, 1165 (2010).

[20] J. Peise, B. Lücke, L. Pezzé, F. Deuretzbacher, W. Ertmer, J. Arlt, A. Smerzi, L. Santos, and C. Klempt, Nat. Commun. **6**, 6811 (2015).

[21] M. Gabbrielli, L. Pezzè, and A. Smerzi, Phys. Rev. Lett. **115**, 163002 (2015).

[22] B. Chen, C. Qiu, S. Chen, J. Guo, L. Q. Chen, Z. Y. Ou, and W. Zhang, Phys. Rev. Lett. **115**, 043602 (2015).

[23] Sh. Barzanjeh, D. P. DiVincenzo, and B. M. Terhal, Phys. Rev. B **90**, 134515 (2014).

[24] C. C. Gerry, Phys. Rev. A **61**, 043811 (2000).

[25] W. N. Plick, P. M. Anisimov, J. P. Dowling, H. Lee, and G. S. Agarwal, New J. Phys. **12**, 113025 (2010).

[26] K. P. Seshadreesan, P. M. Anisimov, H. Lee, and J. P. Dowling, New J. Phys. **13**, 083026 (2011).

[27] C. W. Helstrom, Phys. Lett. A **25**, 101 (1967).

[28] D. F. Walls and G. J. Milburn, *Quantum Optics* (Springer Science & Business Media, New York, 2007).

[29] X. X. Xu and H. C. Yuan, Int. J. Theor. Phys. **53**, 1601 (2014).

[30] R. A. Campos, C. C. Gerry, and A. Benmoussa, Phys. Rev. A **68**, 023810 (2003).

[31] C. C. Gerry, A. Benmoussa, and R. A. Campos, Phys. Rev. A **72**, 053818 (2005).

[32] R. A. Campos and C. C. Gerry, Phys. Rev. A **72**, 065803 (2005).

[33] C. C. Gerry, A. Benmoussa, and R. A. Campos, J. Mod. Opt. **54**, 2177 (2007).

[34] A. Chiruvelli and H. Lee, J. Mod. Opt. **58**, 945 (2011).

[35] C. C. Gerry and J. Mimih, Contemp. Phys. **51**, 497 (2010).

[36] A. Royer, Phys. Rev. A **15**, 449 (1977).

[37] This optimal condition is necessary but not sufficient. Assuming that $\Delta\phi \simeq \Delta\phi_{\mathrm{HL}}$, one can obtain an equation $l_1 N_\alpha^2 + l_2 N_\alpha + l_3 \simeq 0$, where $l_1 = N_{\mathrm{OPA}}^2 + 2N_{\mathrm{OPA}} + 1$, $l_2 = (2N_{\mathrm{OPA}} + 1)^2 N_{\mathrm{s}} + 2N_{\mathrm{OPA}}(N_{\mathrm{OPA}} + 1) - e^{2r} N_{\mathrm{OPA}}(N_{\mathrm{OPA}} + 2)$, and $l_3 = N_{\mathrm{s}}^2(N_{\mathrm{OPA}} + 1)^2 + 2N_{\mathrm{OPA}}(N_{\mathrm{OPA}} + 1)N_{\mathrm{s}} + N_{\mathrm{OPA}}^2 - (N_{\mathrm{s}} + 1)N_{\mathrm{OPA}}(N_{\mathrm{OPA}} + 2)$. Then the necessary optimal condition is found that $N_\alpha = -l_2/(2l_1)$. In the limit of $e^{-g} \to 0$ and $e^{-r} \to 0$, this necessary optimal condition reduces to $N_\alpha \simeq \tanh(2g)e^{2r}/2$.

[38] L. Pezzé and A. Smerzi, Phys. Rev. Lett. **100**, 073601 (2008).

[39] Y. Gao and H. Lee, Eur. Phys. J. D **68**, 1 (2014).

[40] The definition of observable, quadrature, we used here is $\hat{X}_{b_2} \equiv \hat{b}_2^\dagger + \hat{b}_2$. For vacuum inputs, the signal of homodyne detection is always a constant $\langle \hat{X}_{b_2} \rangle = 0$, whereas the variance of signal of homodyne detection is given by $\langle \Delta \hat{X}_{b_2} \rangle \equiv (\langle \hat{X}_{b_2}^2 \rangle - \langle \hat{X}_{b_2} \rangle^2)^{1/2} = \sqrt{4\cosh^2 g \sinh^2 g(1 - \cos\phi) + 1}$, where g is the OPA strength and ϕ is the phase shift. According to the error propagation formula $\Delta\phi_{\mathrm{H}} = \langle \Delta \hat{X}_{b_2} \rangle / |\partial \langle \hat{X}_{b_2} \rangle / \partial \phi|$, one finds that the phase sensitivity is always bad and not available in such a case.

[41] In an SU(2) interferometer with two equal coherent inputs $|i\alpha_0/\sqrt{2}\rangle \otimes |\alpha_0/\sqrt{2}\rangle$, the signal of parity detection is always a constant $\langle \hat{\Pi}_{b_2} \rangle = e^{-2|\alpha_0|^2}$, while the variance of signal of parity detection is also a constant $\langle \Delta \hat{\Pi}_{b_2} \rangle = \sqrt{1 - e^{-4|\alpha_0|^2}}$. According to the error propagation formula $\Delta\phi = \langle \Delta \hat{\Pi}_{b_2} \rangle / |\partial \langle \hat{\Pi}_{b_2} \rangle / \partial \phi|$, the phase sensitivity is always bad and not available in such a case.

[42] S. M. Barnett and P. M. Radmore, *Methods in Theoretical Quantum Optics* (Oxford University Press, Oxford, UK, 2002).

[43] S. L. Braunstein and P. van Loock, Rev. Mod. Phys. **77**, 513 (2005).

[44] C. Weedbrook, S. Pirandola, R. García-Patrón, N. J. Cerf, T. C. Ralph, J. H. Shapiro, and S. Lloyd, Rev. Mod. Phys. **84**, 621 (2012).

[45] A. Monras, arXiv:1303.3682v1.

[46] G. Adesso, S. Ragy, and A. R. Lee, Open Sys. Info. Dyn. **21**, 1440001 (2014).